Sidebands in the Infrared Spectrum of U Centers in Alkali Halides*

JOHN B. PAGE, JR.,† AND B. G. DICK
Department of Physics, University of Utah, Salt Lake City, Utah
(Received 12 May 1967)

A description of the sidebands in the infrared spectrum of crystals containing U centers is presented, together with numerical calculations for the case of U centers in KBr. The sidebands are assumed to arise from the second-order dipole moment and the cubic anharmonicity. Symmetry considerations and the assumption of short-range second-order dipole moment and third-order anharmonic interactions are utilized, and the resulting formulas are evaluated numerically for specific examples within the framework of nearest-neighbor-coupling interactions together with altered harmonic force constants between the defects and their nearest neighbors. It is found within this framework that either the second-order dipole or the cubic anharmonic coupling mechanism can give reasonable agreement with experiment, but that it is always necessary to have a strong decrease in the central force constant between the impurity and its nearest neighbors, as compared with the nearest-neighbor force constant in a pure crystal. This has as its consequence the prediction of a localized mode in the gap between the acoustical and optical frequency branches.

I. INTRODUCTION

THE U center consists of an H^- ion located at a negative-ion vacancy in an alkali-halide crystal. The infrared absorption associated with the high-frequency localized vibrations of these defects was discovered in 1959 by Schäfer.[1] Subsequent theoretical investigations[2–6] have shown that these localized vibrations consist, to a good approximation, of the defect vibrating in a static lattice and that the forces binding the defect are weaker than the corresponding forces in the perfect crystal. More detailed infrared measurements by Fritz and co-workers,[7,8] Timusk and Klein,[9] and Mitra and Brada[10] have revealed well-defined sidebands which are symmetrically located about the main band. At decreasing temperatures the low-frequency sidebands disappear, while the high-frequency sidebands do not. Fritz, Gross, and Bäuerle's[8] measurements of the high-frequency sidebands for U centers in KBr at $T=20°K$ are shown in Fig. 1. Fritz[7] interpreted the sidebands as resulting from the simultaneous excitation of one of the threefold degenerate infrared-active localized modes and absorption or emission of a perturbed band mode—a mode whose frequency lies within the allowed frequency interval of the perfect lattice, but whose associated amplitudes are generally different owing to the loss of translational symmetry as well as to the changed masses and force constants introduced by the defects. Because the unperturbed phonons are well understood in some of the alkali halides through inelastic neutron scattering experiments and their subsequent shell-model interpretation by Cowley *et al.*,[11] the U-center sidebands offer an opportunity to study a relatively simple anharmonic effect and the perturbed vibrations associated with a defect in a crystal whose phonons are known.

In this paper we present a general theoretical description of the U-center sidebands. The formalism splits naturally into three parts which are given in Secs. II–IV. In Sec. II the basic absorption expression is derived assuming that the phonon coupling arises from both the second-order dipole moment and the cubic anharmonicity. In Sec. III the absorption formula is reduced to a physically appealing form by means of symmetry considerations as well as assumptions restricting the extent of the coupling interactions, while in Sec. IV the calculation of those aspects of the perturbed band modes necessary to the theory is briefly discussed. Finally, in Sec. V we present numerical calculations for U centers in KBr.

It will be seen that a knowledge of the unperturbed phonons allows us to calculate the frequency-dependent

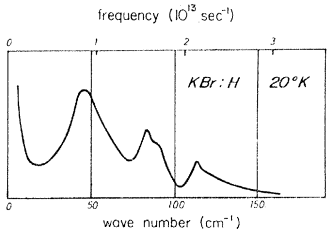

FIG. 1. Fritz *et al.*'s experimental results for the high-frequency, low-temperature sidebands in the infrared spectrum of U centers in KBr. The plotted quantity is proportional to $\ln(I^0/I^u)$, where I^0 and I^u are the transmitted intensities for crystals without and with U centers, and the frequency is measured from the central peak.

* This work was supported by the National Science Foundation.
† Present address: Institut für Theoretische Physik der Universität, Frankfurt/Main, Germany.

[1] G. Schäfer, J. Chem. Phys. Solids **12**, 233 (1960).
[2] H. B. Rosenstock, Phys. Rev. **119**, 1198 (1960).
[3] R. F. Wallis and A. A. Maradudin, Progr. Theoret. Phys. (Kyoto) **24**, 1055 (1960).
[4] S. S. Jaswal and D. J. Montgomery, Phys. Rev. **135**, A1257 (1964).
[5] S. S. Jaswal, Phys. Rev. **140**, A687 (1965).
[6] R. Fieschi, G. F. Nardelli, and N. Terzi, Phys. Rev. **138**, A203 (1965).
[7] B. Fritz, J. Phys. Chem. Solids Suppl. **1**, 485 (1965).
[8] B. Fritz, U. Gross, and D. Bäuerle, Phys. Status Solidi **11**, 231 (1965).
[9] T. Timusk and M. V. Klein, Phys. Rev. **141**, 664 (1966).
[10] S. S. Mitra and Y. Brada, Phys. Letters **17**, 19 (1965).
[11] R. A. Cowley, W. Cochran, B. N. Brockhouse, and A. D. B. Woods, Phys. Rev. **131**, 1030 (1963).

terms in the absorption, provided that we know the changed harmonic force constants associated with the defects. These terms occur with undetermined coupling parameters that must be either calculated independently or guessed. In view of this, we have attempted to learn as much as possible from the computed frequency dependences of the various terms alone.

Timusk and Klein have also made sideband calculations for U centers in KBr, and their model is a special case within the framework given here. Sideband work for U centers in other crystals has been done by Xinh[12] and by Bilz, Strauch, and Fritz,[13] and the relationship of our work to theirs is pointed out at appropriate places in the paper.

II. FORMAL EXPRESSION FOR THE SIDEBAND ABSORPTION

In the experimental work of Fritz *et al.*,[8] with which we will compare our calculations, the sideband shapes and peak positions were found to be independent of the impurity concentration within the range of concentrations studied (10^{-5}–10^{-4}). Accordingly, we will calculate the sideband absorption for the case of a single U center, multiplying the result by the concentration. In addition, it will be assumed that the index of refraction is unaltered by the presence of defects occurring within the above concentration range, so that it will be necessary to calculate only the imaginary part of the electric susceptibility $\chi_I(\omega)$.

Within the Born-Oppenheimer approximation, the interaction between the system and an external electric field which consists of monochromatic plane waves and is switched on adiabatically is

$$-\mathbf{M}\cdot\mathbf{E}e^{-i\omega t}e^{\epsilon t}, \quad \epsilon\to 0^+ \tag{1}$$

where $\mathbf{M}$ is the dipole moment operator of the system and depends upon the system's instantaneous configuration. Assumptions will be made later which will result in confining the interactions responsible for the sideband absorption to a region about the defect that is small compared with the wavelength of the radiation (which is about 20 μ for U centers in KBr), thus justifying the neglect of the spatial variation of the electric field in (1). The formalism of Kubo[14] gives, for a cubically symmetric system subject to the interaction (1), the following expression for the electric susceptibility:

$$\chi(\omega)=\frac{iC}{3\hbar}\int_0^\infty \langle[\mathbf{M}^I(t),\mathbf{M}]\rangle e^{i\omega t}e^{-\epsilon t}dt. \tag{2}$$

In this equation, C is the concentration; $\langle\ \rangle$ denotes a thermal average over the canonical ensemble appropriate to H, the system's Hamiltonian in the absence of an applied field; and $\mathbf{M}^I(t)$, the interaction representation of $\mathbf{M}$, is given by $\exp(iHt/\hbar)\mathbf{M}\exp(-iHt/\hbar)$. Henceforth, $\mathbf{M}^I(t)$ will be written simply as $\mathbf{M}^I$. In the commutator, the scalar product is to be taken. It is convenient to introduce retarded and advanced double-time Green's functions defined by the equations

$$\begin{aligned}\langle\langle\mathbf{M}^I;\mathbf{M}\rangle\rangle_r&=-i\theta(t)\langle[\mathbf{M}^I,\mathbf{M}]\rangle,\\ \langle\langle\mathbf{M}^I;\mathbf{M}\rangle\rangle_a&=i\theta(-t)\langle[\mathbf{M}^I,\mathbf{M}]\rangle,\end{aligned} \tag{3}$$

where $\theta(t)$ is the unit step function. Subtracting these and substituting the result into Eq. (2) gives

$$\chi(\omega)=-\frac{C}{3\hbar}\int_0^\infty \langle\langle\mathbf{M}^I;\mathbf{M}\rangle\rangle_{r,a}e^{i\omega t}e^{-\epsilon t}dt. \tag{4}$$

Here the symbol $\langle\langle\ \rangle\rangle_{r,a}$ stands for the difference $\langle\langle\ \rangle\rangle_r-\langle\langle\ \rangle\rangle_a$. Expressing $\langle\langle\mathbf{M}^I;\mathbf{M}\rangle\rangle_{r,a}$ in terms of its Fourier transform $\langle\langle\mathbf{M}^I;\mathbf{M}\rangle\rangle_{r,a}^\omega$ and making use of the fact that this latter quantity is purely imaginary, we arrive at the following formal expression for the imaginary part of $\chi(\omega)$:

$$\chi_I(\omega)=\frac{iC\pi}{3\hbar}\langle\langle\mathbf{M}^I;\mathbf{M}\rangle\rangle_{r,a}^\omega. \tag{5}$$

If $\mathbf{M}$ is expanded to second order in the normal coordinates d_f, in terms of which H is given by

$$H=\tfrac{1}{2}\sum_f (p_f^2+\omega_f^2 d_f^2)+H_A, \tag{6}$$

where H_A represents the anharmonic potential energy and p_f is equal to $\dot{d}_f$, Eq. (5) becomes

$$\begin{aligned}\chi_I(\omega)=\frac{iC\pi}{3\hbar}\{&\sum_{ff'}\mathbf{M}_f\cdot\mathbf{M}_{f'}\langle\langle d_f^I;d_{f'}\rangle\rangle_{r,a}^\omega\\ &+\tfrac{1}{2}\sum_{ff'f''}\mathbf{M}_f\cdot\mathbf{M}_{f'f''}\\ &\times(\langle\langle d_f^I;d_{f'}d_{f''}\rangle\rangle_{r,a}^\omega+\langle\langle d_f^I d_{f'}^I;d_{f''}\rangle\rangle_{r,a}^\omega)\\ &+\tfrac{1}{4}\sum_{ff'f''f'''}\mathbf{M}_{ff'}\cdot\mathbf{M}_{f''f'''}\langle\langle d_f^I d_{f'}^I;d_{f''}d_{f'''}\rangle\rangle_{r,a}^\omega\}.\end{aligned} \tag{7}$$

Use has been made of the fact that the second-order dipole-moment coupling coefficients $\mathbf{M}_{ff'}$ are symmetric in f and f'. We thus have four $\langle\langle\ \rangle\rangle_{r,a}^\omega$ functions to compute.

In Zubarev's[15] paper it is shown that for any pair of operators, the function $\langle\langle A^I;B\rangle\rangle_{r,a}^\omega$ is equal to

$$\lim_{\epsilon\to 0^+}(\langle\langle A^I;B\rangle\rangle^{\omega+i\epsilon}-\langle\langle A^I;B\rangle\rangle^{\omega-i\epsilon}),$$

where $\langle\langle A^I;B\rangle\rangle^\omega$ is the Fourier transform of the solution to the equations of motion for either $\langle\langle A^I;B\rangle\rangle_r$ or $\langle\langle A^I;B\rangle\rangle_a$, these satisfying the same set of coupled

[12] N. X. Xinh, Solid State Commun. 4, 9 (1966).
[13] H. Bilz, D. Strauch, and B. Fritz, J. Phys. Radium Suppl. 27, C2, 3 (1966).
[14] R. Kubo, J. Phys. Soc. Japan 12, 570 (1957).
[15] D. N. Zubarev, Usp. Fiz. Nauk 71, 71 (1960) [English transl.: Soviet Phys.—Usp. 3, 320 (1960)].

equations. Differentiating the defining equation for $\langle\langle A^I;B\rangle\rangle_r$ twice with respect to t and taking the Fourier transform yields the equations of motion in a form well suited to phonon problems:

$$\omega^2\langle\langle A^I;B\rangle\rangle^\omega=(2\pi\hbar)^{-1}\langle[[A,H],B]\rangle + \hbar^{-2}\langle\langle[[A,H],H]^I;B\rangle\rangle^\omega. \quad (8)$$

In computing each of the four terms in Eq. (7), we will truncate the set (8) by stopping at the lowest sideband-producing order in H_A, for which we will take the following part of the third-order anharmonic potential energy:

$$H_A=\tfrac{1}{2}\sum_{i\alpha\beta}\Phi_{iL\alpha L\beta}d_i d_{L\alpha}d_{L\beta}. \quad (9)$$

Here the $d_{L\alpha}$'s, with α standing for x, y, or z, belong to the threefold degenerate localized mode, i stands for a band mode, and the third-order anharmonic coupling coefficients are the usual third derivatives of the potential energy. When calculated in the above manner, the last term on the right-hand side of (7) gives rise to sidebands in the harmonic approximation, while a sideband contribution is obtainable from the first term only in second order in H_A. These two terms thus represent the limiting cases corresponding to a dominant nonlinear dipole moment or third-order anharmonic (in the sense of our H_A) coupling mechanism. (Of course the nonlinear dipole moment and anharmonic coupling coefficients are not independent, a fact which has been discussed for perfect crystals by Keating and Rupprecht.[16] Nevertheless, the connection between the two kinds of coefficients is complicated and we will therefore carry them through the calculations as parameters.) The second and third terms, representing the intermediate case, turn out to yield sideband contributions to first order in H_A, and the calculation of these "cross terms" will now be briefly sketched.

We first remark that $\langle\langle d_f{}^I;d_{f'}d_{f''}\rangle\rangle^\omega$ will turn out to be an even function of ω and that under this condition the cross terms are equal. To see this, note first that a spectral expansion of the function $\langle\langle B^I(t);A\rangle\rangle_{r,a}$ shows it to be equal to $-\langle\langle A^I(-t);B\rangle\rangle_{r,a}$. Using this we have

$$\langle\langle B^I;A\rangle\rangle_{r,a}{}^\omega=-\langle\langle A^I;B\rangle\rangle_{r,a}{}^{-\omega},$$

from which it follows that $\langle\langle B^I;A\rangle\rangle_{r,a}{}^\omega$ is equal to $\langle\langle A^I;B\rangle\rangle_{r,a}{}^\omega$ whenever $\langle\langle A^I;B\rangle\rangle^\omega$ is even in ω. The contribution to (7) from the cross terms is thus given by

$$\frac{iC\pi}{3\hbar}\sum_{ff'f''}\mathbf{M}_f\cdot\mathbf{M}_{f'f''}\langle\langle d_f{}^I;d_{f'}d_{f''}\rangle\rangle_{r,a}{}^\omega. \quad (10)$$

Furthermore, it turns out that the only terms in this expression which contribute to the sidebands are the ones with f being a localized mode and f' and f'' consisting of a band mode and a localized mode or vice versa. Using $[d_f,p_{f'}]=i\hbar\delta_{ff'}$ to work out the commutators in Eq. (8) for $\langle\langle d_{L\alpha}{}^I;d_{L\beta}d_i\rangle\rangle^\omega$, we obtain

$$\langle\langle d_{L\alpha}{}^I;d_{L\beta}d_i\rangle\rangle^\omega=\hbar\delta_{\alpha\beta}\langle d_i\rangle[2\pi(\omega^2-\omega_L{}^2)]^{-1} + [\omega^2-\omega_L{}^2]^{-1}\sum_{j\gamma}\Phi_{jL\alpha L\gamma}\langle\langle d_j{}^I d_{L\gamma}{}^I;d_{L\beta}d_i\rangle\rangle^\omega. \quad (11)$$

The first term on the right-hand side of this equation gives rise to absorption only at ω_L and will thus be dropped. If we now work out the equations of motion for $\langle\langle d_j{}^I d_{L\gamma}{}^I;d_{L\beta}d_i\rangle\rangle^\omega$ in the *harmonic* approximation, we get a system of two equations, the other unknown being $\langle\langle p_j{}^I p_{L\gamma}{}^I;p_{L\beta}p_i\rangle\rangle^\omega$. Solving these equations, substituting the result into Eq. (11), and simplifying, we get

$$\langle\langle d_{L\alpha}{}^I;d_{L\beta}d_i\rangle\rangle^\omega = \hbar\Phi_{iL\alpha L\beta}[2\pi(\omega^2-\omega_L{}^2)(\omega^2-\omega_+{}^2)(\omega^2-\omega_-{}^2)]^{-1} \times[\langle d_L{}^2\rangle_0(\omega_L{}^2-\omega_i{}^2+\omega^2)+\langle d_i{}^2\rangle_0(\omega_i{}^2-\omega_L{}^2+\omega^2)], \quad (12)$$

where ω_+ and ω_- are $\omega_L+\omega_i$ and $\omega_L-\omega_i$, respectively. $\langle\ \rangle_0$ denotes the thermal average using the harmonic Hamiltonian. Evaluating $\langle\langle\ \rangle\rangle^{\omega+i\epsilon}-\langle\langle\ \rangle\rangle^{\omega-i\epsilon}$ in order to recover $\langle\langle\ \rangle\rangle_{r,a}{}^\omega$ and retaining just those terms which contribute to the sideband absorption at positive ω's we have

$$\langle\langle d_{L\alpha}{}^I;d_{L\beta}d_i\rangle\rangle_{r,a}{}^\omega = -\frac{i\hbar\Phi_{iL\alpha L\beta}}{8\omega_L\omega_i}\left[\left(\frac{\langle d_L{}^2\rangle_0}{\omega_i}+\frac{\langle d_i{}^2\rangle_0}{\omega_L}\right)\delta(\omega-\omega_+) + \left(\frac{\langle d_L{}^2\rangle_0}{\omega_i}-\frac{\langle d_i{}^2\rangle_0}{\omega_L}\right)\delta(\omega-\omega_-)\right], \quad (13)$$

where we have assumed that $\omega_L\gg\omega_i$. Now $\langle d_f{}^2\rangle_0$ is given by $(\hbar/2\omega_f)\coth(\beta\hbar\omega_f/2)$ so that as $T\to 0$ the low-frequency sideband disappears. When the low-temperature limit of (13) is substituted into (10), we see that the cross-term sideband contribution to the imaginary part of the electric susceptibility at $T=0$ is given by

$$\frac{C\pi\hbar}{12\omega_L{}^2}\sum_i\frac{(\sum_{\alpha,\beta}\mathbf{M}_{L\alpha}\cdot\mathbf{M}_{iL\beta}\Phi_{iL\alpha L\beta})}{\omega_i{}^2}\delta(\omega-\omega_+).$$

Proceeding in a similar manner to compute the sideband contributions at $T=0$ from the first and last terms of Eq. (7) for $\chi_I(\omega)$, we obtain the formula

$$\chi_I{}^{\mathrm{SB}}(\omega)=\frac{C\pi\hbar}{12\omega_L}\sum_{i\beta}\frac{1}{\omega_i} \times\left(\frac{\sum_\alpha\mathbf{M}_{L\alpha}\Phi_{iL\alpha L\beta}}{2\omega_L\omega_i}+\mathbf{M}_{iL\beta}\right)^2\delta(\omega-\omega_+), \quad (14)$$

where we have anticipated the result that $\mathbf{M}_{L\alpha}\cdot\mathbf{M}_{L\beta}$ is proportional to $\delta_{\alpha\beta}$. It should be emphasized that the above expression is a perturbation-theoretic result, no

[16] P. N. Keating and G. Rupprecht, Phys. Rev. 138, A866 (1965).

other approximations having been made within our choice of H_A except for the assumption that $\omega_L \gg \omega_i$. Using different methods, Bilz *et al.* have recently derived an expression that is quite similar to Eq. (14), the main difference being the presence of an anharmonically shifted ω_L which was obtained in their calculation by considering higher-order contributions to the absorption. Also, Szigeti[17] has given an analogous relation valid for perfect lattices. The formal result given by Eq. (14) will be the basis for the remainder of this paper.

III. REDUCTION OF THE ABSORPTION FORMULA

Symmetry considerations together with assumptions regarding the localization of the interactions responsible for the sidebands will now be used to bring Eq. (14) to a tractable and more physically meaningful form. First, it is necessary to express the coupling coefficients in terms of the corresponding quantities that occur when the dipole moment and anharmonic potential energy are expanded in powers of particle displacements rather than normal coordinates. Denoting by $\mathbf{u}=\sum_f \chi(f)d_f$ the transformation from the normal coordinates to the configuration-space vector $\mathbf{u}$ representing all of the particle displacements from their equilibrium positions, we see that the coupling coefficients of interest are given by

$$M_{iL\mu}{}^{\alpha}=\sum_{\beta\gamma,lm} M_{\beta\gamma}{}^{\alpha}(l,m)\chi_{\beta}(l|i)\chi_{\gamma}(m|L_{\mu}),$$
$$\Phi_{iL\mu L\nu}=\sum_{\alpha\beta\gamma,lmn} \Phi_{\alpha\beta\gamma}(l,m,n)\chi_{\alpha}(l|i)\chi_{\beta}(m|L_{\mu})\chi_{\gamma}(n|L_{\nu}). \quad (15)$$

Here l, m, etc. refer to particles; α, β, etc. label Cartesian components; and $\{M_{\beta\gamma}{}^{\alpha}(l,m)\}$ and $\{\Phi_{\alpha\beta\gamma}(l,m,n)\}$ are the coefficients appearing in the expansions in terms of the particle displacements. The harmonic part of the Hamiltonian is given in terms of $\mathbf{u}$ by $\frac{1}{2}(\dot{\mathbf{u}}^{\mathrm{T}}\mathbf{M}\dot{\mathbf{u}}+\mathbf{u}^{\mathrm{T}}\mathbf{\Phi}\mathbf{u})$, where $\mathbf{u}^{\mathrm{T}}$ represents the transpose of $\mathbf{u}$, and $\mathbf{M}$ and $\mathbf{\Phi}$ are the mass and harmonic force-constant matrices in configuration space. The $\chi(f)$'s are eigenvectors for the equation

$$(\mathbf{\Phi}-\omega_f{}^2\mathbf{M})\chi(f)=0, \quad (16)$$

which satisfy the completeness and orthonormality conditions

$$\sum_f \mathbf{M}\chi(f)\chi^{\mathrm{T}}(f)=\mathbf{I},$$
$$\chi^{\mathrm{T}}(f)\mathbf{M}\chi(f')=\delta_{ff'}. \quad (17)$$

It is, of course, with the solutions of the harmonic problem (16) for the imperfect lattice that we will ultimately be concerned, but at present the $\chi(f)$'s and ω_f's will be supposed known.

The $\chi(f)$'s may be assumed to be basis functions for irreducible representations of O_h, the point group appropriate to the defect site, and we will use the notation of Bouckaert *et al.*[18] to label the ten irreducible representations. By projecting symmetry coordinates onto the defect site, it is simple to show that the only modes involving motion of the defect are of Γ^{15} symmetry, so that the infrared-active localized mode is of this type and is thus threefold degenerate. In order to determine the band modes for which $M_{iL\mu}{}^{\alpha}$ and $\Phi_{iL\mu L\nu}$ vanish, it is sufficient to learn which irreducible representations are not included in the direct product representation $\Gamma^{15}\times\Gamma^{15}$, this following from the Γ^{15} symmetry of the localized mode and the fact that the dipole moment and potential energy transform as a vector and a scalar under symmetry operations. Using the characters of O_h, one learns that $\Gamma^{15}\times\Gamma^{15}$ contains just the even-parity irreducible representations Γ^1, Γ^{12}, $\Gamma^{15'}$, and $\Gamma^{25'}$, so that Γ^i must be one of these. Furthermore, by using the full irreducible representation matrices plus the fact that $\Phi_{\alpha\beta\gamma}(l,m,n)$ is invariant under permutations of the index pairs (α,l) etc., it can be shown that $\Phi_{iL\mu L\mu}$ is zero when Γ^i is $\Gamma^{15'}$ or $\Gamma^{25'}$ while $\Phi_{iL\mu L\nu}$ for $\mu\neq\nu$ is zero when Γ^i is Γ^1, Γ^{12}, or $\Gamma^{15'}$. The above conclusions are solely a result of symmetry and are thus independent of whatever model assumptions might be made regarding the various quantities appearing in (15).

The observed high frequencies of the localized mode compared with the highest unperturbed lattice frequencies (446 cm^{-1} as opposed to 165 cm^{-1} for U centers in KBr, for instance) indicate that these vibrations are highly localized. Bearing this out are Jaswal's[5] calculations of the ratio of the maximum nearest-neighbor amplitude to that of the impurity for the localized vibrations of U centers in NaCl and KCl, these ratios turning out to be 0.019 and 0.011, respectively. Accordingly, all of the components in $\chi(L_\mu)$ not referring to the impurity will be neglected. Labeling the defect site zero and using the fact that the Γ^{15} symmetry of L_μ results in $\chi_\alpha(0|L_\mu)$ being proportional to $\delta_{\alpha\mu}$ and independent of α, we see that the equations in (15) become

$$M_{iL\mu}{}^{\alpha}=\chi_{\mu}(0|L_{\mu})\sum_{\beta l} M_{\beta\mu}{}^{\alpha}(l,0)\chi_{\beta}(l|i),$$
$$\Phi_{iL\mu L\nu}=\chi_{\mu}{}^2(0|L_{\mu})\sum_{\beta l}\Phi_{\beta\mu\nu}(l,0,0)\chi_{\beta}(l|i). \quad (18)$$

Similarly, it follows that $M_{L\mu}{}^{\alpha}$ is given by $M_{\mu}{}^{\mu}(0)\times\chi_{\mu}(0|L_{\mu})\delta_{\alpha\mu}$, a result which was used in writing Eq. (14) of the last section. From (18) we see that because localized modes are involved in the sideband absorption, the interaction region consists of a volume about the defect of dimensions limited by the range of the dipole moment and anharmonic interactions assumed responsible for the coupling. We will restrict these interactions to the nearest neighbors so that the

[17] B. Szigeti, Proc. Roy. Soc. (London) **A258**, 377 (1960).

[18] L. P. Bouckaert, R. Smoluchowski, and E. Wigner, Phys. Rev. **50**, 58 (1936).

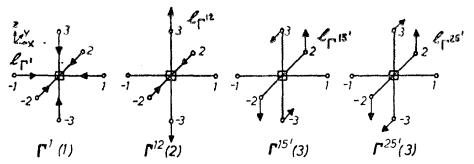

FIG. 2. Components of the $\chi(f)$ vectors on the defect's nearest neighbors for Γ^1, Γ^{12}, $\Gamma^{15'}$, $\Gamma^{25'}$ modes. The degeneracies are given in parentheses.

sums in (18) extend over just the six nearest neighbors of the defect.

To further reduce $M_{iL\mu}{}^{\alpha}$ and $\Phi_{iL\mu L\nu}$, we can determine the form of the $\chi(i)$ vectors in the subspace composed of the defect and its nearest neighbors. This is readily done by means of projection operators, and the results are shown in Fig. 2, which also gives the degeneracy of the modes and the labeling convention. (By reducing the representation obtained by writing down the transformations under symmetry operations of a set of vectors consisting of three orthogonal vectors on each particle, one finds that Γ^1, Γ^{12}, $\Gamma^{15'}$, and $\Gamma^{25'}$ each occur in the nearest-neighbor subspace once and only once. This insures that Fig. 2 is complete.) When the degeneracy is greater than 1, only one partner is drawn. Notice that the basis vectors for each of the four symmetry types is completely specified with but one parameter. This will simplify the work later on.

Finally, point-symmetry considerations can be used to reduce the number of independent elements in $M_{\beta\gamma}{}^{\alpha}(l,0)$ and $\Phi_{\alpha\beta\gamma}(l,0,0)$. Xinh[19] has shown that each of the two kinds of coefficients satisfy a relation like

$$M_{\beta\gamma}{}^{\alpha}(l,0)=\sum_{\alpha'\beta'\gamma'} r_{\alpha'\alpha}r_{\beta'\beta}r_{\gamma'\gamma}M_{\beta'\gamma'}{}^{\alpha'}(l',0)\,,$$

where $\{r_{\alpha'\alpha}\}$ is the three-dimensional orthogonal matrix for a symmetry operation that takes site l to site l'. If l is restricted to the impurity's nearest neighbors and use is made of this relation together with the fact that $\Phi_{\alpha\beta\gamma}(l,0,0)$ is symmetric in β and γ, the following set of independent coupling parameters is obtained:

$$\begin{aligned}
&M_{xx}{}^{x}(1,0)\equiv A\,, \quad \Phi_{xxx}(1,0,0)\equiv A'\,,\\
&M_{yy}{}^{x}(1,0)\equiv B\,, \quad \Phi_{yxy}(1,0,0)\equiv B'\,,\\
&M_{xy}{}^{y}(1,0)\equiv C\,, \quad \Phi_{xyy}(1,0,0)\equiv C'\,,\\
&M_{yx}{}^{y}(1,0)\equiv D\,.
\end{aligned}$$

Xinh has shown, however, that with the coupling interactions restricted to nearest neighbors, the condition of invariance to infinitesimal rotations requires B and D to be equal. This results in a one-to-one correspondence between the independent coupling parameters for each mechanism.

The results of this section can now be used to simplify the basic equation (14) for $\chi_I{}^{\mathrm{SB}}(\omega)$. We will present the results for the limiting cases corresponding to a dominance of either the second-order dipole moment or the third-order anharmonic coupling mechanism, since these will be the cases considered in the numerical work. Converting the band-mode sum in (14) to integrals over the symmetry types that couple with the localized mode and integrating, we arrive at

$$\begin{aligned}
\chi_I{}^{\mathrm{SB}}(\omega_L+\omega)=&\frac{2C\pi h\chi_\mu{}^2(0\,|\,L_\mu)}{3\omega_L\omega}\\
&\times\{\tfrac{3}{2}(A+2C)^2\rho_{\Gamma 1}(\omega)l_{\Gamma 1}{}^2(\omega)\\
&+(A-C)^2\rho_{\Gamma 12}(\omega)l_{\Gamma 12}{}^2(\omega)\\
&+4B^2\rho_{\Gamma 25'}(\omega)l_{\Gamma 25'}{}^2(\omega)\}\quad (19)
\end{aligned}$$

and

$$\begin{aligned}
\chi_I{}^{\mathrm{SB}}(\omega_L+\omega)=&\frac{C\pi h\chi_\mu{}^6(0\,|\,L_\mu)[M_\mu{}^\mu(0)]^2}{6\omega_L{}^3\omega^3}\\
&\times\{\tfrac{3}{2}(A'+2C')^2\rho_{\Gamma 1}(\omega)l_{\Gamma 1}{}^2(\omega)\\
&+(A'-C')^2\rho_{\Gamma 12}(\omega)l_{\Gamma 12}{}^2(\omega)\\
&+4(B')^2\rho_{\Gamma 25'}(\omega)l_{\Gamma 25'}{}^2(\omega)\}\,. \quad (20)
\end{aligned}$$

Equation (19) is the result for the second-order dipole-moment case, and the $\rho_{\Gamma i}(\omega)$ are the densities of states for the band modes of symmetry Γ^i. No contribution from the $\Gamma^{15'}$ modes is present in (19) because of the result that the coupling parameters B and D are equal when the second-order dipole-moment coupling interaction is restricted to nearest neighbors. We see from the above equations that the frequency dependence of the sideband absorption due to the coupling of band modes of a particular symmetry is, apart from a factor of ω^{-1} or ω^{-3} depending upon the particular coupling mechanism under consideration, simply proportional to the product of the appropriate density of states for the imperfect lattice and the corresponding squared (normalized) amplitude of the defect's nearest neighbors. Had the interactions been assumed to extend further, say to the next nearest neighbors, the right-hand sides of (19) and (20) would have contained additional terms, quadratic in the amplitudes of those neighbors included within the range of the interaction. The determination of the $\rho_{\Gamma i}(\omega)$'s and $l_{\Gamma i}{}^2(\omega)$'s will be briefly discussed in the next section.

IV. PERTURBED MODES

The results (19) and (20) of the last section represent the most general form that the absorption formula (14) can take for a light impurity at a site of cubic symmetry under the assumptions of a highly localized mode coupling to the band modes through nearest-neighbor coupling interactions. Our aim is to keep the coupling parameters open, attempting to learn as much as possible from the frequency dependence of the various terms.

[19] N. X. Xinh, Westinghouse Research Laboratories, Pittsburgh, Pennsylvania, Paper No. 65-9F5-442-P8, 1965 (unpublished).

In order to calculate the $l_{\Gamma_i}{}^2(\omega)$'s, we may use the Lifshitz theory of harmonic perturbed lattices, which is reviewed in articles by Dawber and Elliot[20] and Maradudin.[21] In the following outline, the notation will be essentially that of Dawber and Elliot.

Writing the mass and harmonic force-constant matrices as $\mathbf{M}_0+\Delta\mathbf{M}$ and $\mathbf{\Phi}_0+\Delta\mathbf{\Phi}$ where $\mathbf{M}_0$ and $\mathbf{\Phi}_0$ refer to the perfect lattice, one can, for frequencies differing from those of the perfect lattice, rewrite (16) as $\chi(f)=\mathbf{G}^f\mathbf{C}^f\chi(f)$, where $\mathbf{G}^f$ is $(\mathbf{\Phi}_0-\omega_f{}^2\mathbf{M}_0)^{-1}$ and $\mathbf{C}^f$ is $(\omega_f{}^2\Delta\mathbf{M}-\Delta\mathbf{\Phi})$. The perturbed frequencies are the solutions of

$$|\mathbf{I}_{II}-\mathbf{G}_{II}{}^f\mathbf{C}_{II}{}^f|=0. \tag{21}$$

The subscripts refer to the impurity space, defined by those ions for which nonzero elements of $\mathbf{C}^f$ exist. A useful relation, obtained by Sennett,[22] can be obtained by substituting $\mathbf{G}^f\mathbf{C}^f\chi(f)$ for $\chi(f)$ in the orthonormality condition (17) and simplifying the result by means of the identity $\mathbf{G}'^f=\mathbf{G}^f\mathbf{M}_0\mathbf{G}^f$, the prime denoting differentiation with respect to $z\equiv\omega_f{}^2$. The result is

$$[\mathbf{C}_{II}{}^f\chi_I(f)]^\dagger\mathbf{G}'^f{}_{II}[\mathbf{C}_{II}{}^f\chi_I(f)]=1, \tag{22}$$

where a term which drops out whenever f refers to an even-parity mode has been omitted. In terms of the solutions of the dynamical equation (16) for the perfect lattice, $\mathbf{G}^f$ is given by

$$\mathbf{G}^f=\sum_{\mathbf{k},j}\frac{\chi(\mathbf{k},j)\chi^\dagger(\mathbf{k},j)}{\omega_j{}^2(\mathbf{k})-\omega_f{}^2}, \tag{23}$$

the sum extending over the six polarization branches and all of the $\mathbf{k}$ vectors in the Brillouin zone.

We must now choose $\mathbf{C}^f$, the perturbing matrix. It is well known that when the impurity is treated as a mass defect alone, the calculated localized-mode frequencies turn out to be too high. Thus, some of the force constants associated with the defect site must have lower values than in the perturbed crystal. We will describe the force-constant perturbation by means of changed longitudinal and transverse springs connecting the defect with each of its six nearest neighbors. The corresponding spring constant changes will be denoted by δ and γ. Several authors,[9,12,23] both in sideband work and in work on related problems, have used essentially the same model. As Bilz *et al.* have pointed out, such a choice neglects the polarizability of the H^- ion, and this might be important in determining δ and/or γ from the localized-mode data. Nevertheless, for calculating the *even*-parity modes such a choice for the perturbed formal force constants is reasonable and is shown in the Appendix to be consistent with a shell-model description of the system in which the shell-shell force constants between the defect and its nearest neighbors are altered. The fact that within both Timusk and Klein's and our results for KBr, a good description of the sidebands is obtained when the nearest-neighbor force constants are altered by an amount consistent with the observed localized-mode frequencies as treated in the present approximation, indicates that perhaps the contribution to the perturbed force constants from the polarizability might not be very important in this crystal. This question needs further investigation.

TABLE I. Quantities appearing in Eqs. (24) and (25).

Γ^i	$\mathfrak{A}_{\Gamma i}$	$\mathfrak{B}_{\Gamma i}$	$S_{\Gamma i}(z)$
Γ^1	δ	$6\delta^2$	$G_{xx}{}^f(-1,1)-G_{xx}{}^f(1,1)-4G_{xy}{}^f(1,2)$
Γ^{12}	δ	$4\delta^2$	$G_{xx}{}^f(-1,1)-G_{xx}{}^f(1,1)+2G_{xy}{}^f(1,2)$
$\Gamma^{25'}$	γ	$4\gamma^2$	$G_{yy}{}^f(-1,1)-G_{xx}{}^f(1,1)-2G_{xy}{}^f(1,2)$

Equations (21) and (22) for the even-parity modes which can couple with the localized mode may now be written down, the work being simplified by using symmetry arguments to reduce the form of $\mathbf{G}^f$ in the impurity space. We find that the frequency and squared-amplitude equations can in each of the three cases be written as

$$1=\mathfrak{A}_{\Gamma i}S_{\Gamma i}(z), \tag{24}$$

and

$$l_{\Gamma i}{}^2(z)=-[\mathfrak{B}_{\Gamma i}dS_{\Gamma i}(z)/dz]^{-1}, \tag{25}$$

with $\mathfrak{A}_{\Gamma i}$, $\mathfrak{B}_{\Gamma i}$, and $S_{\Gamma i}(z)$ being given in Table I.

Now Eq. (25) must be evaluated at the z's corresponding to the solutions of (24), and this is formally the same problem as evaluating the squared amplitude at the defect site for Γ^{15} motion with no perturbed force constants. Dawber and Elliot and Maradudin have discussed the latter problem and just the results will be quoted here. Maradudin writes $S(z)$ as $(1/3N)\times\sum_\rho\theta(\rho)/(z-\lambda_\rho)$, where $\{\lambda_\rho\}$ is the set of distinct unperturbed $\omega_j{}^2(\mathbf{k})$'s. The equation $\lambda_\rho=z$ defines both $\rho(z)$ and $\theta[\rho(z)]$ as continuous functions of z, in terms of which a function $G(z)\equiv\theta(z)\rho'(z)/3N$ is introduced. The number of points in the Brillouin zone is N. It is then possible to express Eqs. (24) and (25) in terms of $\theta(z)$ and $G(z)$ and to combine these equations to yield

$$l_{\Gamma i}{}^2(z)=\frac{\mathfrak{A}_{\Gamma i}{}^2\theta_{\Gamma i}(z)}{\mathfrak{B}_{\Gamma i}3N\{[1-\mathfrak{A}_{\Gamma i}\tilde{G}_{\Gamma i}(z)]^2+\mathfrak{A}_{\Gamma i}{}^2\pi^2G_{\Gamma i}{}^2(z)\}}, \tag{26}$$

where $\tilde{G}(z)$ is the Hilbert transform of $G(z)$. Equation (26) now expresses $l_{\Gamma i}{}^2$ in terms of smoothly varying, readily calculable quantities. Approximate forms of $\theta(z)$ and $G(z)$ may be easily computed by averaging them over Δz intervals which are small enough to include the important frequency dependences of these quantities but which still contain many λ_ρ's. For the latter condition to hold, we must be sure to know the unperturbed solutions at a sufficiently large number of points in the Brillouin zone.

[20] P. G. Dawber and R. J. Elliot, Proc. Roy. Soc. (London) **A273**, 222 (1963).
[21] A. A. Maradudin, in *Phonons and Phonon Interactions*, edited by T. A. Bak (W. A. Benjamin, Inc., New York, 1964), p. 424.
[22] C. T. Sennett, thesis, Oxford University, 1964 (unpublished).
[23] C. T. Sennett, J. Phys. Chem. Solids **26**, 1097 (1965).

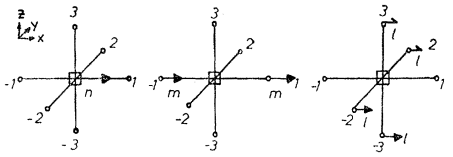

FIG. 3. Illustrating one partner from each of the three types of Γ^{15} modes which can occur in the impurity space.

Turning to the perturbed densities of states for the various symmetry types, we will assume that these are the same as the corresponding densities in the perfect crystal and that these, in turn, are related to the total unperturbed density of states through the relation

$$\rho_{\Gamma i}(\omega)=d_{\Gamma i}{}^2\rho_0(\omega)/h+O(N^{-1/3}),$$

$d_{\Gamma i}$ being the dimensionality of Γ^i and h being the order of the point group. Knox[24] has shown that the $(d_{\Gamma i})^2/h$ factors give the fraction of the total number of states of each symmetry type. For the modes of interest here we thus have $\rho_{\Gamma 1}=\rho_0/48$, $\rho_{\Gamma 12}=\rho_0/12$ and $\rho_{\Gamma 25'}=3\rho_0/16$. Actually, our assumption that the $\rho_{\Gamma i}$'s are the same in the perturbed and unperturbed crystal needs to hold only within the intervals Δz that we use in the computation of $\theta(z)$ and $G(z)$. In view of Rayleigh's theorems, which state that a given perturbed frequency will not be shifted past its adjacent unperturbed frequencies, our assumption should be valid again as long as there are a sufficient number of λ_ρ's within each Δz.

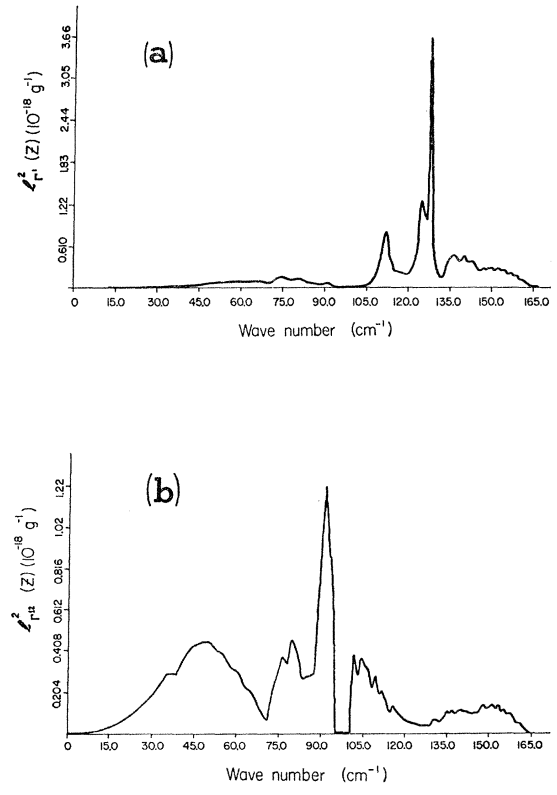

FIG. 4. Squared amplitudes (normalized) of the defect's nearest neighbors for (a) Γ^1 modes and (b) Γ^{12} modes with $\delta=-8.87\times10^3$ dyn cm^{-1}. A localized mode occurring in the gap at 96 cm^{-1} has been suppressed in (b), as explained in Sec. V.

[24] R. S. Knox, Solid State Commun. 4, 453 (1966).

Within our choice of $\mathbf{C}^f$, we can obtain an expression relating its elements to the localized-mode frequency. Symmetry arguments similar to those of Sec. III show that three Γ^{15} modes, each being threefold degenerate, occur within the impurity space. One partner from each type is shown in Fig. 3, and it will be assumed that the localized mode is a linear combination of these three. With this choice for $\chi(L_x)$, the frequency condition (21) yields a 3×3 determinantal condition in δ and γ. For the $\gamma=0$ case, it is possible to express δ as a function of ω_L:

$$\delta=(G_1\omega_L{}^2\Delta m-1)\times\{\Delta m\omega_L{}^2[2G_4{}^2-G_1(G_2+G_3)]+G_2+G_3+2G_1-4G_4\}^{-1}. \quad (27)$$

The Green's functions appearing here are $G_1=G_{xx}{}^f(0,0)$, $G_2=G_{xx}{}^f(1,1)$, $G_3=G_{xx}{}^f(-1,1)$, and $G_4=G_{xx}{}^f(0,1)$. An approximate form for (27), obtained by making use of Fieschi *et al.*'s argument that only the (0,0) elements of $\mathbf{C}^f$ need be retained when treating localized modes whose frequencies are well above the maximum of the unperturbed lattice frequencies, has been used by Timusk and Klein and yields for the $\gamma=0$ case the result

$$\delta\approx(G_1\omega_L{}^2\Delta m-1)/2G_1. \quad (28)$$

We will find this to be an excellent approximation for U centers in KBr.

When γ is not zero, a similar approximation leads to the same relation with δ replaced by $\delta+2\gamma$.

V. NUMERICAL RESULTS AND CONCLUSIONS

Given the eigenvalues and eigenvectors for the perfect lattice plus values for δ and γ, we can now compute the frequency dependence of the various terms appearing in Eqs. (19) and (20). Calculations have been performed by us for U centers in KBr, using model VI of Cowley *et al.*'s shell model since it reproduces accurately the measured phonon dispersion curves in KBr and NaI. Unfortunately, U-center data for NaI are currently unavailable, so we have confined our attention to KBr. The frequencies and eigenvectors were evaluated at 1686 points in Kellerman's 1/48 section of the Brillouin zone, this being equivalent to 64 000 points after applying symmetry operations. One hundred Δz intervals were used so that each interval contained approximately $6\times16.86\approx100$ distinct frequencies.

The anharmonic coupling used in Timusk and Klein's sideband calculation for U centers in KBr can be obtained from the model presented here by setting all of the second-order dipole-moment coupling parameters equal to zero, as well as all of the anharmonic parameters

TABLE II. Comparison of the experimental[a] peak positions and peak-height ratios with those calculated for coupling through $\Phi_{xxx}(1,0,0)$ only.

Peak	Peak positions Calculated (cm^{-1})	Observed (cm^{-1})	Error (%)
1	43.0	44.9	−4.2
2	82.0	82.2	−0.54
3	112.0	113.0	−0.62

Ratio	Peak-height ratios Calculated	Observed	Error (%)
P_1/P_2	4.22	1.45	191.0
P_1/P_3	8.94	2.73	227.0
P_2/P_3	2.12	1.88	12.7

[a] Reference 8.

except $\Phi_{xxx}(1,0,0)\equiv A'$. Equation (20) then gives, up to a constant factor,

$$\chi_I^{SB}(\omega_L+\omega)\propto[l_{\Gamma 1}^2(\omega)+(8/3)l_{\Gamma 12}^2(\omega)]\rho_0(\omega)\omega^{-3}. \quad (29)$$

We wish to compare the results so obtained with those corresponding to the analogous formula for the second-order dipole case, namely, the one that results from neglecting all of the coupling parameters in (19) except $M_{xx}^x(1,0)\equiv A$. The result, again up to a constant factor, is just (29) with ω^{-3} replaced by ω^{-1}. To determine δ for this comparison we shall use the observed ω_L value of 446 cm^{-1} in Eq. (27), which yields the result $\delta=-8.87\times10^3$ dyn cm^{-1} with γ equaling zero. Timusk and Klein used the approximation (28) and obtained a value for δ of -9.25×10^3 dyn cm^{-1}. Thus in this case, Fieschi *et al.*'s approximation is excellent.

Using our value of δ, we can compute $l_{\Gamma 1}^2(\omega)$ and $l_{\Gamma 12}^2(\omega)$ as described earlier. The results are shown in Fig. 4. The peaks near 127 cm^{-1} in $l_{\Gamma 1}^2(\omega)$ are caused by the vanishing of $[1-\delta G_{\Gamma 1}(z)]$ and thus correspond to pseudolocalized modes. As discussed by Timusk and Klein, a large change in the nearest-neighbor force constant such as we have used here (our δ corresponds to a value of 0.41 for Timusk and Klein's parameter η, which measures the ratio of $-\delta$ to the nearest-neighbor central repulsive force constant of shell model VI) leads to the prediction of a localized mode of Γ^{12} symmetry in the gap between the acoustical and optical modes of the host lattice. This mode occurs even for small force-constant changes ($\eta>0.16$), and we have suppressed it for computational reasons in Fig. 4(b) and in subsequent figures where it occurs.

Combining the density of states with $l_{\Gamma 1}^2(\omega)$ and $l_{\Gamma 12}^2(\omega)$ according to (29) and the analogous relation for the second-order dipole coupling, we calculate the curves shown in Fig. 5. The curves for $\delta=0$ are included in order to illustrate the large improvement brought about by the force-constant change. The small peak near 10 cm^{-1} in Fig. 5(b) is probably due to the lack of a fine enough mesh of Brillouin-zone points for the contributions in this frequency region. Figure 5(b) corresponds to the lower curve in Timusk and Klein's Fig. 7, and by comparing it with our Fig. 5(a) we see that within the models under examination here, the anharmonic coupling mechanism yields better agreement with experiment than does that due to the second-order dipole moment. In Table II the measured peak positions and height ratios from Fig. 1 for the three principal peaks are compared with the calculated values from Fig. 5(b). Notice that although the theory yields good peak positions, the calculated height ratios are in poor agreement with the observed ones.

As discussed by Bilz *et al.*, theoretical sideband calculations by them for U centers in KCl using a density approximation, i.e., neglecting the frequency dependence of the $\alpha(f)$ vectors, resulted in a dominance of the anharmonic over the second-order dipole coupling mechanism. In addition, Xinh,[12] after assuming that the coupling interactions are central in character and have a specific form came to the same conclusion regarding the dominant coupling for U centers in KI. We will shortly see that when the coupling parameters are left open, good over-all agreement (in the sense of peak height ratios as well as peak positions) for U

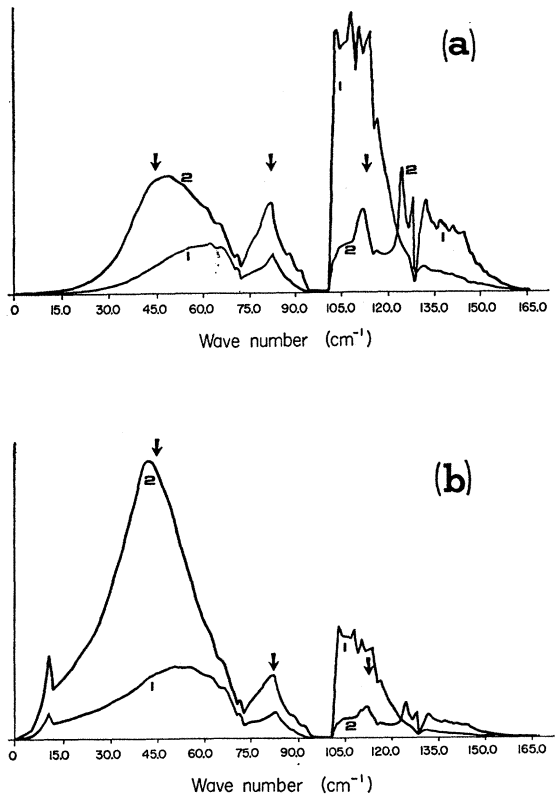

FIG. 5. Calculated sideband absorption (to within a constant factor) assuming (a) just second-order dipole coupling through $M_{xx}^x(1,0)$, and (b) just third-order anharmonic coupling through $\Phi_{xxx}(1,0,0)$. Curves 1 and 2 in each case represent the results for $\delta=0$ and $\delta=-8.87\times10^3$ dyn cm^{-1}, respectively, and the arrows give the frequencies of the three principal sidebands as measured by Fritz. As in Fig. 4, the localized mode in the gap has been suppressed.

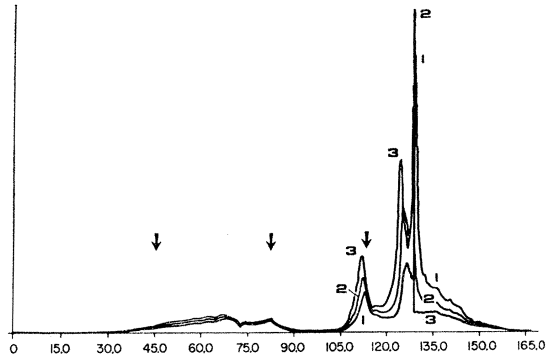

FIG. 6. Calculated sideband contribution (to within a constant factor) from the Γ^1 modes assuming a dominant second-order dipole coupling. The plotted quantity is $l_{\Gamma^1}{}^2(\omega)\rho_0(\omega)/\omega$ and the δ values are: (1) -5×10^3 dyn cm^{-1}; (2) -7×10^3 dyn cm^{-1}; (3) -9×10^3 dyn cm^{-1}.

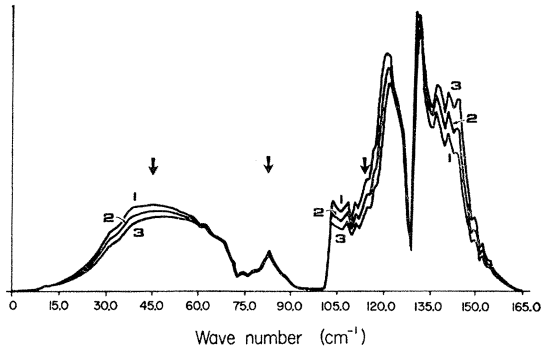

FIG. 8. Calculated sideband contribution (to within a constant factor) from the $\Gamma^{25'}$ modes assuming a dominant second-order dipole coupling. The plotted quantity is $l_{\Gamma25'}{}^2(\omega)\rho_0(\omega)/\omega$ and curves 1, 2, and 3 correspond to values for γ of -2×10^3, -1×10^3, and 0 dyn cm^{-1}, respectively.

centers in KBr can be obtained from the second-order dipole contributions. This indicates that care must be taken to justify any particular model for the coupling interactions before using sideband calculations to draw conclusions regarding the relative importance of each type of coupling.

A comparison of Figs. 4 and 5 shows that the structure of $l_{\Gamma1}{}^2$ in the optical phonon region gives rise to some of the nonobserved features of the theoretical sidebands of Fig. 5(b). In view of this and because the present theory leaves the coupling parameters open, we have computed the frequency dependence of each of the three terms in (19) and the three terms in (20) separately for different values of δ and γ with an aim towards determining the relative importance to the sideband absorption of the different symmetry types of perturbed phonons. The results are given in Figs. 6 through 11. The first thing we note is that the curves for the "transverse" modes, the $\Gamma^{25'}$'s, do not give much indication of being important. This is not surprising, since the coupling parameter for these modes should be less than those for the "longitudinal" Γ^1 and Γ^{12} modes. Secondly, we see that except for the predicted peak near 112 cm^{-1}, the curves for the Γ^1 modes bear little resemblance to the experimental results. Unfortunately, the 112-cm^{-1} peak is always accompanied by additional peaks occurring near 127 cm^{-1}, which are unobserved and are due to pseudolocalized modes. Focusing now upon the Γ^{12} modes, we see that most of the good agreement of curve 5(b) is due to the contributions of these modes. Notice the dependency of the first sideband peak upon δ and that for either mechanism a strong change in this quantity is necessary. Of the curves shown, we see that the second curve in Fig. 10 ($\eta=0.33$) gives the best over-all agreement for the anharmonic case, but that the peak-height ratios are still poorly represented. On the other hand, curve 3 of Fig. 7, giving the contribution to the absorption from the second-order dipole coupled Γ^{12} modes for $\delta=-9\times10^3$dyn cm^{-1} ($\eta=0.42$) removes most of the peak-height discrepancy while retaining good agreement for the peak positions. The peak-height ratios and positions for this curve are given in Table III. The shape of the curve for frequencies below that of the first peak is not as appealing as the shape of the curve of Fig. 5(b) in this region.

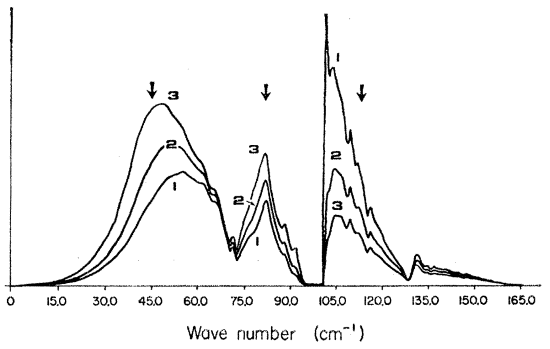

FIG. 7. Same as Fig. 6 but for the Γ^{12} contributions, given by $l_{\Gamma12}{}^2(\omega)\rho_0(\omega)/\omega$. Gap modes at 100, 98, and 96 cm^{-1} for curves 1, 2, and 3 have been omitted.

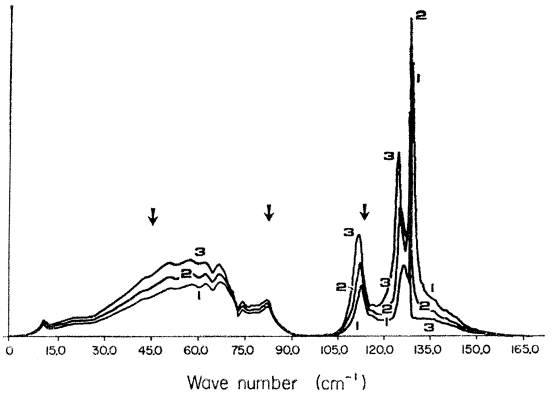

FIG. 9. Calculated sideband contribution (to within a constant factor) from the Γ^1 modes assuming a dominant third-order anharmonic coupling. The curves are ω^{-2} times those of Fig. 6.

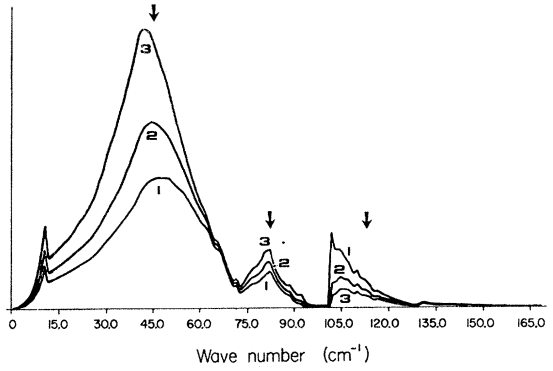

FIG. 10. Same as Fig. 9 but for the Γ^{12} contributions. The curves are ω^{-2} times those of Fig, 7.

TABLE III. Calculated peak positions and peak-height ratios for the second-order dipole coupled Γ^{12} contributions.

Peak	Peak positions Calculated (cm^{-1})	Error (%)
1	49.0	8.6
2	82.0	−0.24
3	105.0	−6.8
	Peak-height ratios	
Ratio	Calculated	Error (%)
P_1/P_2	1.36	−6.2
P_1/P_3	2.44	−11.9
P_2/P_3	1.79	−5.2

From the results shown in Figs. 6 through 11 we thus conclude that, within the restrictions of nearest-neighbor coupling interactions and our choice of the perturbed force constants, the Γ^{12} modes are primarily responsible for the main sideband in KBr, that comparatively large values of δ ($\eta=0.3$–0.4) give the best agreement with experiment for either coupling mechanism, and that one cannot unequivocally determine the dominant coupling mechansim from calculations of just the frequency dependence of the sidebands without *a priori* knowledge of the coupling parameters. (Regarding the question of coupling mechanisms, another type of argument has been given in Ref. 13, where it has been pointed out that the observed temperature independence of the infrared U band's oscillator strength indicates that the dominant coupling is anharmonic.) Furthermore, the values of δ needed to obtain good agreement are consistent with the value ($\eta=0.41$) calculated from the observed localized-mode frequency by neglecting γ and the polarizability of the defect.

Notice that the anharmonic coupling parameters $(A'+2C')^2$ and $(A'-C')^2$ for the Γ^1 and Γ^{12} modes are quite sensitive to changes in the relative magnitudes of A' and C'. In particular, if C' is 10% of A' and is of the opposite sign, the ratio of $(A'+2C')^2$ to $(A'-C')^2$ has a value of 0.53 instead of 1.0, the value assumed by Timusk and Klein. A similar result holds, of course, for the corresponding second-order dipole moment coupling parameters. Again we see the necessity of making careful *a priori* estimates of the coupling parameters.

The necessity of using strongly perturbed longitudinal force constants (shell-shell—see Appendix) between the impurity and its nearest neighbors in order to obtain good agreement with experiment also implies the existence of a localized mode in the gap, as we have mentioned. This gap mode is of the same symmetry (Γ^{12}) as the modes which have been seen to be the most important in the sideband absorption. Though this mode is not itself infrared active, it should be observable in the sideband absorption, as discussed by Timusk and Klein. The possibility of eliminating this discrepancy from the theory by including coupling interactions to the next nearest neighbors has been suggested by Bilz *et al.*, and from the results presented here it is clear that it cannot be eliminated in a satisfactory way from a model which includes just nearest-neighbor coupling interactions together with altered harmonic force constants between the defect and its nearest neighbors.

Nevertheless, most of the observed features of the sidebands in KBr can, as we have seen, be quantitatively accounted for within the framework given here.

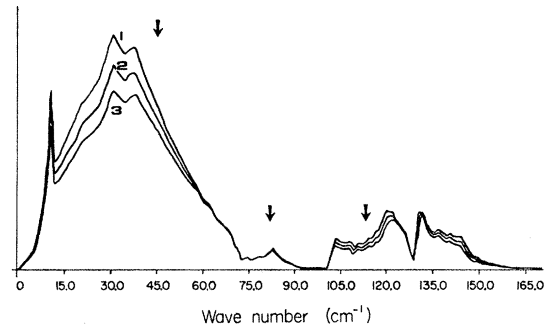

FIG. 11. Calculated sideband contribution (to within a constant factor) from the $\Gamma^{25'}$ modes assuming a dominant third-order anharmonic coupling. The curves are ω^{-2} times those of Fig. 8.

ACKNOWLEDGMENTS

The authors wish to acknowledge helpful discussions with Dr. M. Klein and Professor H. Bliz concerning their sideband work. One of us (J. B. P.) especially thanks Professor Bilz and the Institut für Theoretische Physik, Frankfurt, for their hospitality during the writing of this paper.

APPENDIX: SHELL-MODEL TREATMENT OF THE PERTURBED PHONONS

In the shell model, the formal force-constant matrix $\mathbf{\Phi}$ is given by $\mathbf{\Phi}_{cc}-\mathbf{\Phi}_{cs}\mathbf{\Phi}_{ss}^{-1}\tilde{\mathbf{\Phi}}_{cs}$, where $\mathbf{\Phi}_{cc}$, $\mathbf{\Phi}_{cs}$, and $\mathbf{\Phi}_{ss}$ are matrices representing the core-core, core-shell, and

shell-shell interactions. Now for the Lifshitz theory to be useful, a perturbing matrix $\mathbf{C}^f=\omega_f^2\Delta\mathbf{M}-\Delta\mathbf{\Phi}$ is needed which is nonzero only in a relatively small impurity space. But because of the presence of the $\mathbf{\Phi}_{cs}\mathbf{\Phi}_{ss}^{-1}\tilde{\mathbf{\Phi}}_{cs}$ term, it is not clear that localized changes in the shell-model parameters lead to only localized changes in $\mathbf{\Phi}$. We can avoid this difficulty by employing shell as well as core eigenvectors in a Lifshitz-type formalism. In the shell model, the fundamental equation for the perturbed vibrations may be written as

$$\begin{pmatrix}\chi_c(f)\\ \chi_s(f)\end{pmatrix}=\begin{pmatrix}\mathbf{G}_{cc}^f & \mathbf{G}_{cs}^f\\ \tilde{\mathbf{G}}_{cs}^f & \mathbf{G}_{ss}^f\end{pmatrix}\times\begin{pmatrix}\omega_f^2\Delta\mathbf{M}_{cc}-\Delta\mathbf{\Phi}_{cc} & \Delta\mathbf{\Phi}_{cs}\\ \Delta\tilde{\mathbf{\Phi}}_{cs} & \Delta\mathbf{\Phi}_{ss}\end{pmatrix}\begin{pmatrix}\chi_c(f)\\ \chi_s(f)\end{pmatrix},\quad\text{(A1)}$$

where the elements of the Green's function matrix are given by

$$\mathbf{G}_{cc}^f=\sum_{\mathbf{k},j}\frac{\chi_c(\mathbf{k},j)\chi_c^\dagger(\mathbf{k},j)}{\omega_j^2(\mathbf{k})-\omega_f^2},\quad \mathbf{G}_{cs}^f=\sum_{\mathbf{k},j}\frac{\chi_c(\mathbf{k},j)\chi_s^\dagger(\mathbf{k},j)}{\omega_j^2(\mathbf{k})-\omega_f^2},$$

and

$$\mathbf{G}_{ss}^f=\sum_{\mathbf{k},j}\frac{\chi_s(\mathbf{k},j)\chi_s^\dagger(\mathbf{k},j)}{\omega_j^2(\mathbf{k})-\omega_f^2}+\mathbf{\Phi}_{0ss}^{-1},$$

all quantities referring to the perfect lattice. The $\chi_c(\mathbf{k},j)$'s are identical to the $\chi(\mathbf{k},j)$'s of Eq. (23), and the $\chi_s(\mathbf{k},j)$'s are the corresponding unperturbed shell eigenvectors, measured from the shell equilibrium positions. The symmetry reduction of $\chi_c(f)$, $\chi_s(f)$, $\mathbf{G}_{cc}^f$, $\mathbf{G}_{cs}^f$, and $\mathbf{G}_{ss}^f$ is similar to that given in the formal force-constant picture. For the sidebands, we are concerned with just the even-parity modes and can thus neglect the long-range changes in $\mathbf{\Phi}_{cc}$, $\mathbf{\Phi}_{cs}$, and $\mathbf{\Phi}_{ss}$ induced by the altered core and shell charges of the defect, provided that we neglect relaxation effects. Describing the short-range force-constant changes by longitudinal and transverse spring-constant changes, δ_s and γ_s, between the defect's shell and those of its nearest neighbors, we have a localized impurity space within which to apply Eq. (A1). For the even-parity modes it is easily shown that within our impurity space, the perturbed-shell eigenvectors satisfy the normalization condition

$$\chi_s^{\mathrm{T}}(f)\mathbf{C}_{ss}^f\mathbf{G'}_{ss}^f\mathbf{C}_{ss}^f\chi_s(f)=1,\quad\text{(A2)}$$

the prime denoting differentiation with respect to $z\equiv\omega_f^2$.

Working out the frequency and amplitude conditions for the even-parity modes, we arrive at equations identical with Eqs. (24) and (25) except that δ and γ are replaced by δ_s and γ_s, l is replaced by l_s, and all of the Green's functions are shell-shell Green's functions. For each symmetry type we also have an equation relating the shell and core amplitudes on the defect's nearest neighbors. For example, for Γ^{12} modes this condition is

$$l_c=l_s\delta_s[G_{csxx}^f(-1,1)-G_{csxx}^f(1,1)+2G_{csxy}^f(1,2)].$$

We can now use the methods outlined in the main body of the paper to calculate $l_c^2(\omega)$ and hence the absorption for the different symmetry types and for different values of δ_s and γ_s. When this is done it turns out that, except for a factor, the resulting curves are essentially identical to those previously given. The refinements included in the shell-model formalism, therefore, do not make any non-negligible changes in our earlier conclusions. Thus, as far as the even-parity modes are concerned, the changed nearest-neighbor formal force constants can be identified with the changed shell-shell force constants between the impurity and its nearest neighbors.

These results are undoubtedly due to the fact that in the unperturbed lattice, the isotropic core-shell spring constants are much greater than the shell-shell force constants. This results in $\mathbf{\Phi}_{0ss}^{-1}$ being unimportant in $\mathbf{G}_{ss}^f$ at the band-mode frequencies and in the unperturbed core and shell eigenvectors being very nearly always proportional. Thus $\mathbf{G}_{cs}^f$ and $\mathbf{G}_{ss}^f$ are essentially just multiples of $\mathbf{G}_{cc}^f$, in which case the results reduce, but for a factor, to those given by the formal theory.